https://doi.org/10.18485/resylab.2024.6.ch1

Multi-source data analysis in slow-moving landslide-affected built-up environment: case studies in Calabria region (southern Italy)

Dario Peduto[(1)*], Gianfranco Nicodemo[(1)], Davide Luongo[(1)], Settimio Ferlisi[(1)], Luigi Borrelli[(2)], Diego Reale[(3)], Gianfranco Fornaro[(3)], Giovanni Gullà[(2)]

1) Department of Civil Engineering, University of Salerno, Via Giovanni Paolo II, 132, 84084 - Fisciano (SA), Italy (dpeduto@unisa.it, gnicodemo@unisa.it, dluongo@unisa.it, sferlisi@unisa.it)

2) Research Institute for Geo-Hydrological Protection (CNR-IRPI), National Research Council of Italy, Via Cavour n. 4/6, 87030, Cosenza, Italy (borrelli@irpi.cnr.it; giovanni.gulla@irpi.cnr.it)

3) Institute for Electromagnetic Sensing of the Environment (IREA – CNR), National Research Council of Italy, Via Diocleziano 328, 80124 Naples, Italy (reale.d@irea.cnr.it; fornaro.g@irea.cnr.it)

Abstract The paper deals with a key step of slow-moving landslide risk analysis such as the vulnerability estimation of the interacting facilities (e.g., buildings, roads) via the exploitation of multi-source multi-temporal data. These latter include information gathered from conventional multi-source (geological, geomorphological and geotechnical) data, which are integrated with non-invasive spaceborne remote sensing monitoring (e.g., Differential Interferometric techniques), in-situ and virtual surveying (e.g., Google Street view imagery). The approach proposed in this work relies on the methodological frameworks developed by the authors within a 20-year multidisciplinary research activity. Two case studies in Calabria region (southern Italy) affected by several slow-moving landslides, which caused damage to the built environment, were selected. The analysis of the available monitoring data allowed i) characterizing slow-moving landslides and ii) generating predictive tools for estimating the degree of loss (inherently related to the expected damage) of the exposed facilities. Once further validated, the proposed circular approach could be part of a procedure for prioritizing building/road (extraordinary) maintenance activities and scheduling/implementing risk mitigation measures.

Keywords slow-moving landslides, circular approach, built-up environment, monitoring/surveying data, damage, risk, buildings, roads.

Introduction

Landslides yearly cause huge losses worldwide in terms of consequences on either people (i.e., injury and life losses) or the built-up environment (i.e., damages of different severity levels to structures and infrastructure).

The analysis of consequences induced by a landslide represents a key step for estimating the risk to which people and/or (infra)structures interacting with a landslide are (or can be) exposed (Fell et al., 2008). Focusing on slow-moving landslides, consequence analysis involves identifying/quantifying the structures (i.e., buildings) and/or the infrastructures (i.e., roads) at risk as well as estimating their vulnerability (Peduto et al., 2017; Argyroudis et al., 2019). This latter depends on both the landslide intensity (in terms of spatially-distributed parameter related to the landslide destructiveness) and peculiar features of the exposed facilities (e.g., geometry, material properties, state of maintenance, structural and foundation typology for buildings). Therefore, its estimation is a difficult task that entails a thorough knowledge of both the landslide mechanisms (Mavrouli et al. 2014; Peduto et al., 2018) and the behaviour of the exposed elements (Ferlisi et al., 2019) as well as the monitoring of landslide intensity parameters (Peduto et al., 2017).

Nowadays, the technological innovation in monitoring systems (both ground-based or remotely operating) offers the concrete possibility to access unprecedented rich datasets that the landslide community can profitably use for risk analysis purposes. In this regard, the present paper aims at providing an example of how multi-source monitoring/surveying conventional or innovative data can complement with each other to enhance vulnerability analysis and/or forecasting capabilities in the field of landslide consequence analysis.

Proposed approach

The approach proposed to investigate the vulnerability of structures and infrastructures in landslide-affected urban areas includes three main phases (Fig. 1).

The first phase (Phase I) pursues the detection of the elements at risk (i.e. buildings and/or road networks). According to the scale of analysis, quality and resolution of the used data (Ferlisi et al., 2019), they are identified by overlapping base and thematic maps (e.g., built-up area map, DEM, landslide inventory map) with available observations (e.g., optical imagery) and/or monitoring (i.e., provided by conventional or innovative field/remote monitoring techniques) data (Peduto et al., 2018; Greenwood et al., 2019).

In Phase II, a damage severity level (DL) as well as a value of the intensity parameter (IP) are assigned to every identified exposed element. In particular, the DL is classified based on the analysis of field and/or remote surveys adopting a proper damage ranking. The selected IP (e.g., velocity, settlement or related parameters) is computed based on the quality and resolution of available monitoring data.

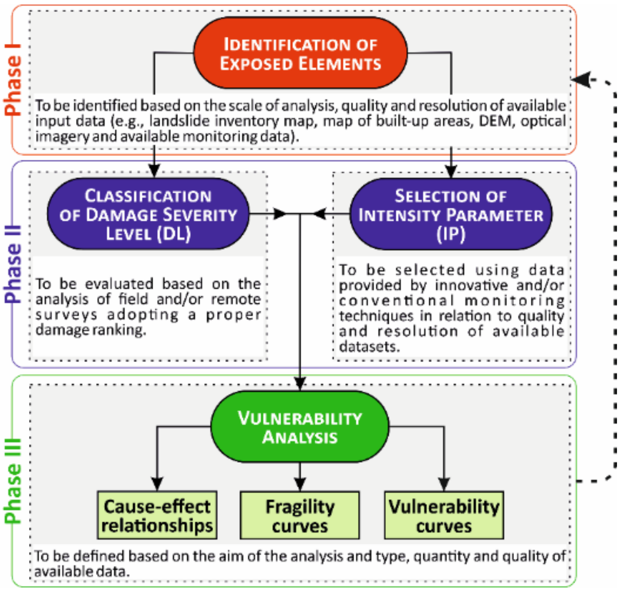

Fig. 1 Flowchart of the proposed approach (Peduto et al., 2021).

In Phase III, the recorded DL and the retrieved magnitude of IP are combined to analyse the vulnerability of the exposed elements.

For this purpose, data are treated based on the aim of the study (i.e., in relation to the scale of analysis), the type (i.e., empirical or numerical) of the analysis, the quantity and quality of available data, via deterministic (i.e., intended to investigate the established relationships between the cause (IP) and effect (DL)) or probabilistic (i.e., aimed at generating consequence forecasting tools such as fragility and/or vulnerability curves) approaches (Ferlisi et al., 2019).

Particularly, DInSAR-derived IP can be first merged with the recorded DLi to retrieve the cause (IP) - effect (DL) relationship; then, according to the procedure described by Peduto et al. (2017, 2018), assuming the log-normal distribution function as probabilistic model, empirical fragility curves providing the conditional probability for a randomly selected building/road section at risk to be in, or exceed, a certain DL when the IP equals a given value can be generated via Eq.(1):

$$P(\text{Damage} \geq \text{DLi}|\text{IP}) = \Phi\left[\frac{1}{\beta_i}\ln\frac{\text{IP}}{\overline{\text{IP}}}\right] \quad (1)$$

where the fragility parameters associated with the standard normal cumulative distribution function Φ[.] are the median value of the selected intensity parameter ($\overline{\text{IP}}$) and the standard deviation (β_i) of the natural logarithm of the (IP) values.

Then, the vulnerability curve can be used to quantitatively link the expected average level of damage severity (μ_{DL}) and the IP (Eq.2) considering for each DLi the discrete probability (Pi) retrieved from the previously generated fragility curves with an associated numerical index *di* (ranging from 0 to 1 according to DLi).

$$\mu_{DL}(\text{IP}) = \sum_{i=1}^{3} P_i * d_i (2)$$

Finally, using the tangent hyperbolic function (Lagomarsino and Giovinazzi, 2006) as regression model to fit the empirical data, the empirical vulnerability curve, which relates the expected mean level of damage severity (μ_D) to a given exposed element to an IP value, can be derived (Eq. 3).

$$\mu_D = a[b + \tanh(c * \text{IP} + d)] \quad (3)$$

where a, b, c and d are four coefficients determined for the investigated sample of elements at risk using the least mean square method.

Results

Two well-documented case studies in Calabria region (southern Italy) were analysed. As for buildings, the urban centre of the Lungro town, which has been extensively suffering from several slope instabilities that caused damage of different severity to the built-up area, was selected. The SS660 road, which is affected by several ground displacements that over time have caused frequent closures to vehicle traffic, was chosen as test infrastructure. It consists of a 7 m-wide single carriageway with two traffic lanes that represent the main access to Acri town.

Lungro case study

The urban area of Lungro (Fig. 2), located at 650 m a.s.l. in the northern sector of the Calabria region, presents a complex geological context in which the Lungro-Verbicaro Unit dating back to the Middle Trias made up of metapelites and metacarbonates prevails (Gullà et al., 2017). The urban centre is widely affected by slow-moving landslides with either active or dormant state based on geomorphological criteria (Fig. 2a).

Consequently, over the years, several damages (Fig. 2a) were recorded to both masonry buildings – mainly located in the historic centre and its surroundings (Carmine and Lafcantino), made up of 2–3 floors with pebbles, or erratic/irregular stones on shallow foundations – and reinforced concrete buildings up to 5–6 floors mainly located in the San Leonardo area, built since the early 1950–1960s (Peduto et al., 2017, 2018).

Previous studies in the area (Gullà et al., 2017) typified the inventoried slow-moving landslides in six categories (Fig. 2a), through the application of the "aPosIn" procedure that relies on the combination of geological information, geomorphological criteria and both geotechnical and remote displacement monitoring data. These categories differ for geometric and kinematic characteristics, involved soils, and type of movement.

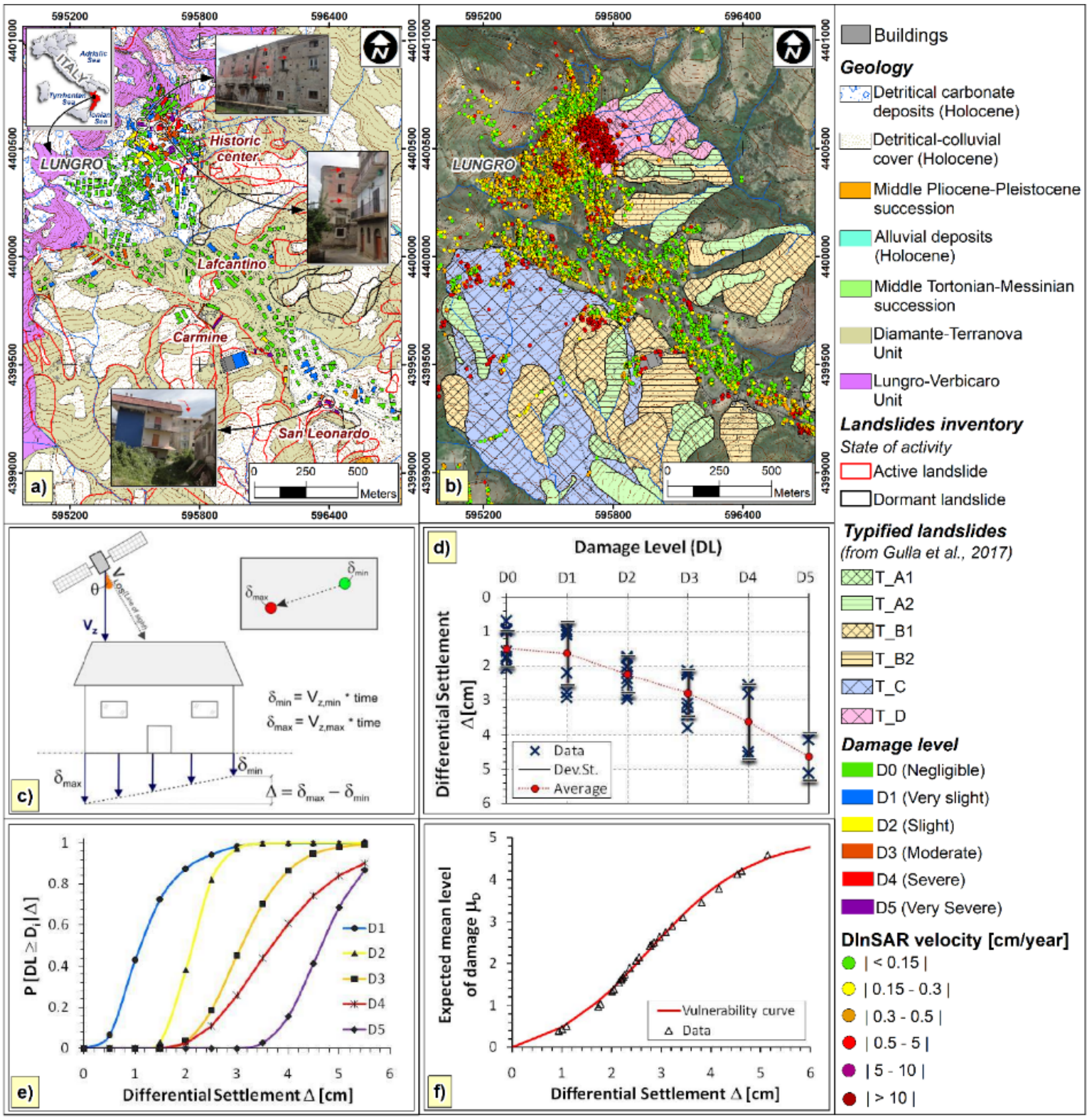

Fig. 2 Lungro case study: a) geological and landslide inventory maps along with their state of activity (modified from Gullà et al., 2017) and building damage map with some examples of crack patterns exhibited by both reinforced concrete and masonry buildings (modified from Peduto et al., 2017); b) map of typified landslides with spatial distribution of DInSAR data acquired by COSMO-SkyMed satellite (ascending orbit, 2012–2014) (modified from Gullà et al., 2017 and Peduto et al., 2018); c) sketch of the DInSAR-derived differential settlement (Δ) of a building; d) damage level (DLi) vs. differential settlements (Δ); e) empirical fragility curves and f) vulnerability curve for masonry buildings in Lungro area (Peduto et al., 2021).

In the area, in addition to deep and surface displacement monitoring data deriving from conventional (inclinometers and GPS) techniques (Gullà et al., 2017; Peduto et al., 2018), innovative monitoring data provided by the interferometric processing of spaceborne synthetic aperture radar images (DInSAR) acquired by Envisat (period August 2003 to January 2010) and COSMO-SkyMed (period October 2012 to April 2014) radar sensors are available. Fig. 2b shows the spatial distribution of the DInSAR coherent pixel velocities derived from the processing of COSMO-SkyMed images on ascending orbit, which were processed according to the SAR tomographic analysis (Fornaro et al., 2009) which proved to be particularly effective for monitoring built-up areas (Peduto et al., 2017, Nicodemo et al., 2018).

Following the described approach (Fig. 1), in Phase I, single buildings exposed to landslide risk were identified by combining the available input data. Then, in Phase II, both DL and IP were estimated. The former was assigned to each single building (Fig. 2a) based on the data collected via ad-hoc predisposed building fact-sheets (Ferlisi et al., 2015; Peduto et., 2017) during an extensive in-situ damage survey carried out in October 2015 (including the whole urban area over a total of 540 buildings). The recorded DLs were categorized by adapting the classification system proposed by Burland et al. (1977) on the basis of the visual interpretation of crack patterns exhibited by the building façades considering six categories (D0 = negligible; D1 = very slight; D2 = slight; D3 = moderate; D4 = severe; D5 = very severe). The IP was assumed as the differential settlement (Δ) computed using the DInSAR data on 49 exposed single buildings (12 of reinforced concrete and 37 of masonry structure) out of 111 total buildings interacting with slow-moving landslides; for this purpose, only those buildings covered by at least two coherent DInSAR benchmarks in both Envisat and COSMO-SkyMed datasets were considered. The DInSAR-derived differential settlement (Δ) was computed as the maximum difference (Fig. 2c) of the cumulative settlements (δ, derived by multiplying the DInSAR velocity along the vertical direction for the observation period of both available SAR datasets) recorded by the DInSAR benchmarks within the building perimeter (Peduto et al., 2017). In the last phase (Phase III), referring to 37 masonry buildings composing a homogeneous sample (i.e., masonry 2-3 floored structures on shallow foundations) and exhibiting all the different damage severity levels (i.e., from D1 to D5), the building vulnerability was investigated. First, Fig. 2d shows a generally increasing trend of DL when Δ increases. Then, empirical fragility curves for randomly selected buildings at risk in Lungro town were generated using Eq. 1 (Fig. 2e) by estimating the fragility parameters pertaining to each DLi. Finally, the empirical vulnerability curve (Fig. 2f) was derived by interpolating, using the Eq. 3, the values of the averagely expected damage severity level (μ_{DL}) derived through the adoption of the Eq. 2 with a numerical index *di* equal to 0.2, 0.4, 0.6, 0.8 and 1 for D1, D2, D3, D4 and D5, respectively.

State Road SS660 case study

The study area, located along the western border of the Sila Massif (northern sector of the Calabria region), falls within the middle portion of the Mucone River basin and includes the town of Acri (Fig. 3). The climate is Mediterranean with dry summer and precipitation concentrated during mild winters (Terranova et al. 2007). The area, ranging in elevation from 300 to 900 m a.s.l., is made by high-grade metamorphic rocks of Palaeozoic age, which result intensely weathered (Borrelli et al. 2007; Borrelli et al. 2014). Landslides (Fig. 3a, b) (mainly active and dormant slide-debris flows, debris slides, and rockslides) are widespread along the Mucone River, where the local relief energy, steep slopes, and gravitational landforms are commonly associated with fault zones. Landslides can be distinguished in three categories (i.e. shallow, medium-deep, and deep-seated) based on geomorphological criteria (Borrelli and Gullà 2017), Figure 3b. In addition, a large Deep-Seated Gravitational Slope Deformation of Sackung-type (Serra di Buda DSGSDs) affects the study area (Borrelli and Gullà 2017), Figure 3a, b. This DSGSD, with a depth equal or higher than 200 m, has a length of about 1.2 km, a width of 3 km and a surface of 3 km^2. The typical features of this phenomenon, partially covered by shallow, medium-deep and deep landslides, are summit crown-shaped scarps, terrace-like flats, convex slope profiles, and foot protrusions towards the bed of the watercourses. The geomaterials (Fig. 3b) produced by weathering and degraded processes of the gneissic rocks in the study area and in similar geological context can be framed among residual-colluvial soils to saprolitic soils (Cascini and Gullà 1993); their connection with tectonic sub-horizontal structures favour the formation of deep-seated failure surfaces, as in the case of Serra di Buda slow-moving landslide. In Phase I, the road stretch exposed to landslide risk was identified by combining the available input data (Fig. 3a). Then, in Phase II, both IP and DL and were estimated. Particularly, PS velocity values (Fig. 3a) were projected from the LOS to the steepest slope direction following the procedure proposed by Cascini et al. (2010), also fixing a threshold of 4 to the projection coefficient of the 1750 projected PSs for COSMO-SkyMed dataset over the SS660. Then, starting from the landslide inventory map reported in Borrelli and Gullà (2017) and focusing on the Serra di Buda slope, the landslides in the area were typified (Fig. 3b). A multi-temporal analysis of the damage was carried out and the recorded damage was ranked in four increasing DLi (D0 = negligible; D1 = slight; D2 = moderate; D3 = severe) including both the asphalt pavement (see Ferlisi et al. 2021) and the side retaining structures for the cut-and-fill slope sections of the SS660. Referring to the results of the in-situ survey carried out on 14 December 2021, 69 damaged sections were identified and distinguished according to the severity level recorded to both the asphalt pavement and the side retaining structures. Some photos of the most damaged locations are shown in Fig. 3c. The map in Fig. 3b shows the lengths of the sections with uniform levels of damage that were computed by dividing in two parts the distance between two damaged sections and attributing them the DLi of the closest damaged section in the observation period. The availability of multi-temporal damage data revealed that the damage mainly concentrated in the Serra di Buda rockslide due to its reactivation in 2005 and 2010 (Gullà 2014). In the period 2011 - 2021, a replacement of the road surface was carried out as revealed by the archive photos systematically acquired by the IRPI-CNR. To estimate the IP, first a buffer with a radius of 10 m was drawn around each damaged road section and the PSs located within its perimeter were selected; then, the mean slope velocity of the k_{th} buffer was computed as the root mean square weighted PS velocity along the steepest slope direction (as proposed by Cascini et al. 2013). The cumulative displacement (δ_{slope}) pertaining to k_{th} buffer was assumed as the IP and computed by multiplying the velocity value for the observation period (t).

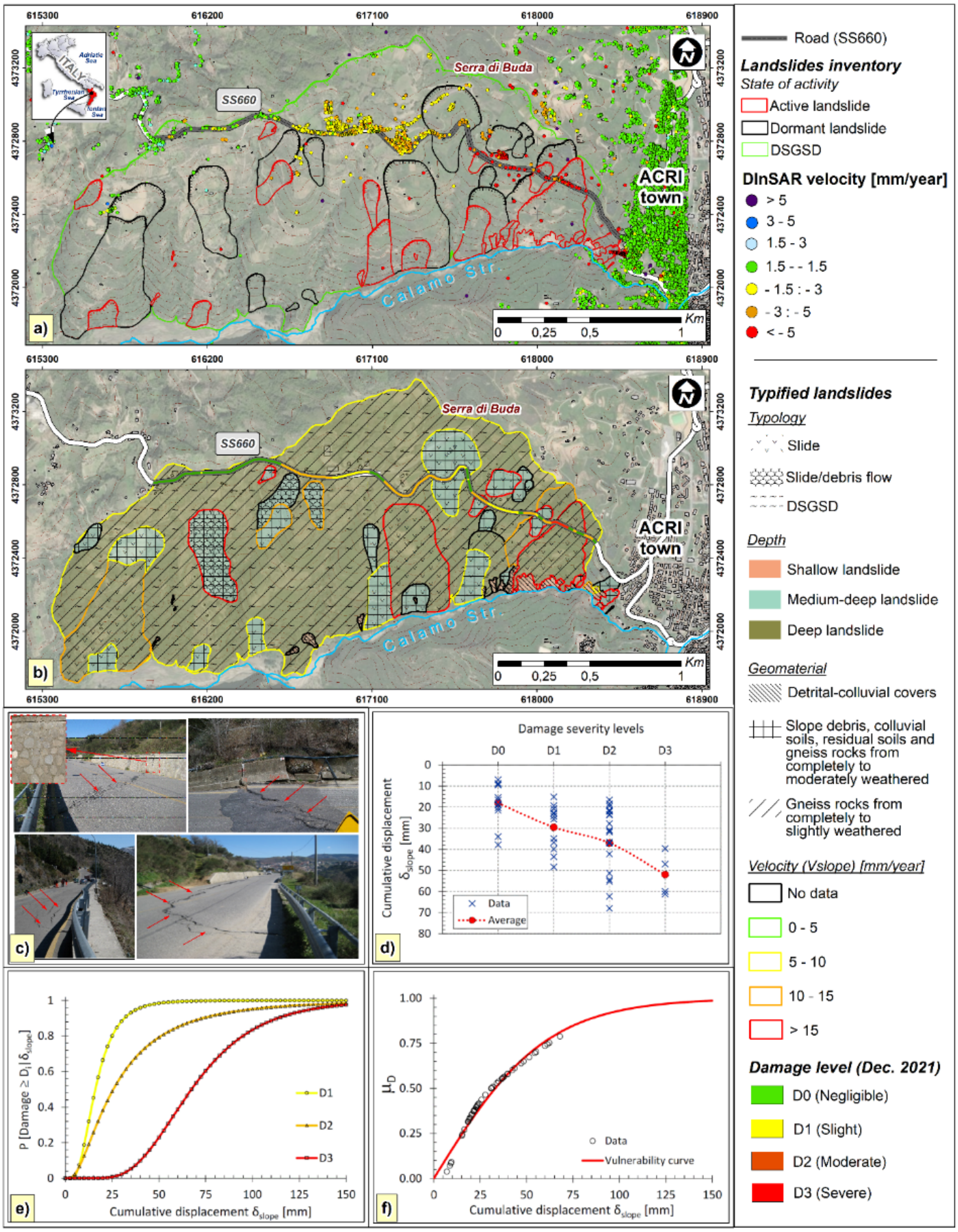

Fig. 3 State Road SS660 case study: a) landslide inventory map with the state of activity (modified from Borelli and Gullà et al., 2017), the analyzed (SS660) road to Acri town, and spatial distribution of DInSAR data acquired by COSMO-SkyMed satellite (ascending orbit, 2014–2021); b) map of the typified landslides with indication of damage to road; c) some examples of cracks recorded on the asphalt pavement and the side retaining structures during in-situ surveys; d) damage level (DLi) vs. cumulative displacement (δ_{slope}); e) empirical fragility curves and f) vulnerability curve.

Specifically, displacements were cumulated from February 2018 (coinciding with the last repair works to the road) to December 2021. The computed values of δ_{slope} for each buffer were then associated with the DLi recorded in the survey of 2021. This allowed retrieving the empirical cause-effect relationship shown in Figure 3d.

As expected, the δ_{slope} attains higher values as the damage severity level (DLi) increases, being DLi conservatively assumed as the most severe damage between the one recorded to the road surface and the pertaining retaining structure (if any).

Then, by adopting Eq. 1 with the estimated fragility parameters pertaining to each DLi, the empirical fragility curves were generated (Figure 3e).

Finally, the discrete probabilities (Pi) provided by the empirical fragility curves allowed deriving - according to Eq. 2 - the values of the average expected damage severity level (μ_{DL}), assuming as numerical index *di* the values 0.33, 0.66, and 1 for D1, D2 and D3, respectively.

The interpolation of the latter empirical data through the adoption of Eq. 3 allowed deriving the empirical vulnerability curve shown in Figure 3f.

Discussion and Conclusions

The presented case studies showed that technological innovation of multi-source monitoring/survey data can provide useful contribution to procedures aimed at landslide risk analyses. For instance, Google Street View was proven to be a useful tool for rapid, easy and cost-effective road damage inspections, whereas DInSAR data confirmed to be a well-established complement of conventional displacement monitoring techniques. Both the abovementioned datasets, which are broadly available in archives worldwide, can foster deterministic/probabilistic vulnerability analyses of buildings/roads exposed to slow-moving landslides.

Once further validated, the presented method could be part of a circular approach (Gullà et al., 2021) to help building/road maintenance prioritization and scheduling as well as risk management in slow-moving landslide-affected urban area and extended to other geo-hazards. Nevertheless, the exportability to other areas will require updated landslide inventories, local geotechnical and building/road characteristics to be taken into account to typify representative landslide-damaged buildings/roads in homogeneous geo-lithological contexts.

Acknowledgements

This research was funded by and carried out in the Italian Space Agency (ASI) contract n. 2021–10-U.0 CUP F65F21000630005 MEFISTO—Multi-frequency SAR data processing methods for the hydrogeological instability monitoring.

The activities also fall within the Agreement for scientific cooperation signed by the Italian National Research Council (CNR-IRPI) and the Department of Civil Engineering of the University of Salerno on "*Attività di ricerca mirate ad approfondire le conoscenze sulla tipizzazione di movimenti franosi a cinematica lenta e sulla vulnerabilità di strutture e infrastrutture che con essi interagiscono anche mediante l'impiego di tecniche innovative di monitoraggio satellitare e da terra*" and the related operative Agreement for Research contribution signed by the two institutions on the topic: "*Analisi quantitativa del rischio da frane a cinematica lenta in aree urbane dell'Appennino Meridionale con l'ausilio di modellazione numerica avanzata e dati di monitoraggio satellitare*".

References

Argyroudis S A, Mitoulis S A, Winter M G, Kaynia A M (2019) Fragility of transport assets exposed to multiple hazards: State-of-the-art review toward infrastructural resilience. Reliability Engineering and System Safety, 191:106567, doi: 10.1016/j.ress.2019.106567.

Borrelli L, Gullà G (2017) Tectonic constraints on a deep-seated rock slide in weathered crystalline rocks. Geomorphology 290: 288–316. https://doi.org/10.1016/j.geomorph.2017.04.025

Borrelli L, Greco R, Gullà G (2007) Weathering grade of rock masses as a predisposing factor to slope instabilities: Reconnaissance and control procedures. Geomorphology 87(3): 158–175. https://doi.org/10.1016/j.geomorph.2006.03.031

Borrelli L, Perri F, Critelli S, Gullà G (2014) Characterization of granitoid and gneissic weathering profiles of the Mucone River basin (Calabria, southern Italy). Catena 113: 325–340. https://doi.org/10.1016/j.catena.2013.08.014

Burland J B, Broms B B, de Mello V F B (1977) Behaviour of foundations and structures. Proceedings of the 9th Int. Conf. on Soil Mechanics and Foundation Engineering, Tokyo. SOA Report, vol. 2, pp. 495–546.

Cascini L, Gullà G (1993) Caratterizzazione fisico-meccanica dei terreni prodotti dall'alterazione di rocce gneissiche. Rivista Italiana di Geotecnica, Anno XXVII, N. 2, Aprile-Giugno 1993, pp.125-147 (in Italian).

Cascini L, Fornaro G, Peduto D (2010) Advanced low- and full-resolution DInSAR map generation for slow-moving landslide analysis at different scales. Engineering Geology, 112(1–4):29-42. https://doi.org/10.1016/j.enggeo.2010.01.003

Fell R, Corominas J, Bonnard Ch, Cascini L, Leroi E, Savage W Z (2008) Guidelines for landslide susceptibility, hazard and risk zoning for land-use planning. Engineering Geology 102(3-4):99-111. https://doi.org/10.1016/j.enggeo.2008.03.014

Ferlisi S, Gullà G, Nicodemo G, Peduto D (2019) A multi-scale methodological approach for slow-moving landslide risk mitigation in urban areas, southern Italy. Euro-Mediterranean Journal for Environmental Integration, 4:20, doi:10.1007/s41207-019-0110-4

Ferlisi S, Marchese A, Peduto D (2021) Quantitative analysis of the risk to road networks exposed to slow-moving landslides: a case study in the Campania region (southern Italy). Landslides 18:303–319. https://doi.org/10.1007/s10346-020-01482-8

Ferlisi S, Peduto D, Gullà G, Nicodemo G, Borrelli L, Fornaro G (2015) The use of DInSAR data for the analysis of building damage induced by slow-moving landslides. Engineering Geology for Society and Territory - Landslide Processes, © Springer International Publishing - Vol. 2. pp. 1835–1839. doi: 10.1007/978-3-319-09057 3_325.

Fornaro G, Pauciullo A, Serafino F (2009) Deformation monitoring over large areas with multipass differential SAR interferometry: A new approach based on the use of spatial differences. Int J Remote Sens 30(6):1455–1478. https://doi.org/10.1080/01431160802459569

Greenwood W W, Lynch J P, Zekkos D (2019) Applications of UAVs in civil infrastructure. Journal of Infrastructure Systems, 25(2):04019002.

Gullà G (2014) Field monitoring in sample sites: hydrological response of slopes with reference to widespread landslide events. Procedia Earth and Planetary Science 9 (2014) 44-53.

Gullà G, Nicodemo G, Ferlisi S, Borrelli L, Peduto D (2021) Small-scale analysis to rank municipalities requiring slow-moving landslide risk mitigation measures: the case study of the Calabria region (southern Italy). Geonvironmental Disasters (2021) 8:31.

Gullà G, Peduto D, Borrelli L, Antronico L, Fornaro G (2017) Geometric and kinematic characterization of landslides affecting urban areas: the Lungro case study (Calabria, southern Italy). Landslides. 14(1):171–188.

Lagomarsino S, Giovinazzi S (2006) Macroseismic and mechanical models for the vulnerability and damage assessment of current buildings. Bull Earthq Eng 4(4):415-443. https://doi.org/10.1007/s10518-006-9024-z

Mavrouli O, Fotopoulou S, Pitilakis K, Zuccaro G, Corominas J, Santo A, Cacace F, De Gregorio D, Di Crescenzo G, Foerster E, Ulrich T (2014) Vulnerability assessment for reinforced concrete buildings exposed to landslides. Bull Eng Geol Environ 73:265– 289. https://doi.org/10.1007/s10064-014-0573-0

Nicodemo G, Peduto D, Ferlisi S, Gullà G, Reale D, Fornaro G (2018) DInSAR data integration in vulnerability analysis of buildings exposed to slow-moving landslides. In: Proceedings of IEEE International Geoscience and Remote Sensing Symposium (IGARSS 2018), Valentia (Spain), 22-27 July, 2018, pp. 6111-6114. https://doi.org/10.1109/IGARSS.2018.8518808

Peduto D, Ferlisi S, Nicodemo G, Reale D, Gullà G (2017) Empirical fragility and vulnerability curves for buildings exposed to slow-moving landslides at medium and large scales. Landslides. 14(6):1993–2007.

Peduto D, Nicodemo G, Caraffa M, Gullà G (2018) Quantitative analysis of consequences induced by slow-moving landslides to masonry buildings: a case study. Landslides. 15(10):2017–2030

Peduto D, Nicodemo G, Nappo N, Gullà G (2021) Innovation in Analysis and Forecasting of Vulnerability to Slow-Moving Landslides. In: Guzzetti F., Mihalić Arbanas S., Reichenbach P., Sassa K., Bobrowsky P.T., Takara K. (eds) Understanding and Reducing Landslide Disaster Risk. WLF 2020. ICL Contribution to Landslide Disaster Risk Reduction. Volume 2 "From Mapping to Hazard and Risk Zonation", pp.441-446. Springer, Cham. https://doi.org/10.1007/978-3-030-60227-7_51, Print ISBN978-3-030-60226-0, Online ISBN978-3-030-60227-7, © Springer Nature Switzerland AG 2021

Terranova O, Antronico L, Gullà G (2007) Landslide triggering scenarios in homogeneous geological contexts: the area surrounding Acri (Calabria, Italy). Geomorphology 87: 250-267 https://doi.org/10.1016/j.geomorph.2006.09.021